Hopf Bifurcation and Chaos in Simplest Fractional-Order Memristor-based Electrical Circuit

Mohammed-Salah Abdelouahab, René Lozi

Published in
Indian Journal of Industrial and Applied Mathematics
Vol. 6, Issue 2, July-December 2015, pp. 105-109
DOI: 10.5958/1945-919X.2015.00009.2 personal file

Hopf Bifurcation and Chaos in Simplest Fractional-Order Memristor-based Electrical Circuit

Mohammed-Salah Abdelouahab[1] and René Lozi[2*]
[1]Associate Professor, Laboratory of Mathematics and their Interactions, Mila University Center, Mila, Algeria
[2]Professor, University of Nice-Sophia Antipolis, Laboratory of Mathematics J. A. Dieudonné, U.M.R. CNRS 7351, Parc Valrose, Nice, 06108 Cedex 02, France
(*Corresponding Author) E-mail Id: *rlozi@unice.fr; [1]m.abdelouahab@centre-univ-mila.dz

Abstract: In this article, we investigate the bifurcation and chaos in a simplest fractional-order memristor-based electrical circuit composed of only three circuit elements: a linear passive capacitor, a linear passive inductor and a non-linear active memristor with two-degree polynomial memristance and a second-order exponent internal state. It is shown that this fractional circuit can exhibit a drastically rich non-linear dynamics such as a Hopf bifurcation, coexistence of two, three and four limit cycles, double-scroll chaotic attractor, four-scroll chaotic attractor, coexistence of one (or two) chaotic attractor with one limit cycle and new chaotic attractor which is not observed in the integer case. Finally, the presence of chaos is confirmed by the application of the recently introduced 0–1 test.

Keywords: Fractional derivative, Memristor, Chaos, Electrical circuit, Hopf bifurcation, Dynamical system, Strange attractor

1. INTRODUCTION

The fractional calculus is more than 300 years old with the first written note dated to 1695 [1]. Several physical phenomena can be described more accurately by fractional differential equations rather than integer-order models [2]. In the past, the lack of methods for solving fractional differential equations was the reason for using only integer-order models. Nowadays, a number of techniques are available for approximating fractional derivatives and integrals [3]. There are several definitions of fractional derivatives and integrals [4], for example for a sufficiently smooth function f:

The Riemann–Liouville fractional integral of order $\alpha > 0$ is given by

$$J_a^\alpha f(t) = \frac{1}{\Gamma(\alpha)} \int_a^t (t-s)^{\alpha-1} f(s) ds, \quad t > a$$

The Riemann–Liouville fractional-order derivative ${}^{RL}_{a}D^{\alpha}_{t} f$ is defined by

$${}^{RL}_{a}D^{\alpha}_{t} f = D^{m} J^{m-\alpha}_{a} f, \quad m = \lceil \alpha \rceil ,$$

The Caputo fractional-order derivative $_aD^{\alpha}_{t} t$ is defined by

$${}_{a}D^{\alpha}_{t} f(t) = J^{m-\alpha}_{a} D^{m} f(t), \quad m = \lceil \alpha \rceil ,$$

The Grünwald–Letnikov fractional-order derivative is given by

$${}^{GL}_{a}D^{\alpha}_{t} f(t) = \lim_{h \to 0} h^{-\alpha} \sum_{k=0}^{\frac{t-a}{h}} (-1)^{k} \left(\frac{\Gamma(\alpha+1)}{k!\Gamma(\alpha-k+1)} \right) f(t-kh).$$

Fractional-order derivatives of a periodic function cannot be a periodic function [5], as a consequence of this property; the time-invariant fractional-order systems do not have any non-constant periodic solution. In [6], it is proposed a solution for this problem by imposing a simple modification to the Grünwald–Letnikov definition.

Memristor is a new electrical element which has been predicted and described in 1971 by Chua [7] and for the first time realised by HP laboratory in 2008 [8].

Chua proved that memristor behaviour could not be duplicated by any circuit built using only the other three elements (resistor, capacitor and inductor) (see Figure 1(a)).

In [9], we have generalised the definition of fractance (which was first introduced in 1983) and after that introduced the paradigm of memfractance which is fitted for circuit elements with memory such as memristor, meminductor, memcapacitor and second-order memristor. We have defined a new element called memfractor which possesses interpolated characteristics between those four circuit elements and proved a generalised Ohm's law. Due to the non-linearity of memristor element, memristor-based circuits can easily generate a chaotic signal. In 2010, Muthuswamy and Chua

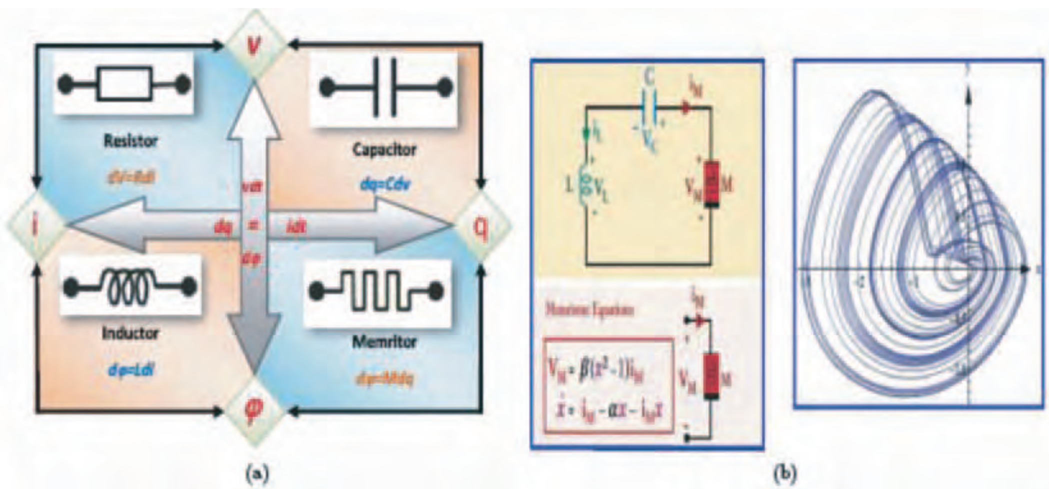

Figure 1. (a) Four basic circuit elements. (b) Circuit schematic and the one-scroll chaotic attractor from [10].

[10] proposed a memristor-based circuit comprising only three elements: a linear passive inductor, a linear passive capacitor and a non-linear active memristor with a second-degree polynomial memristance,

$$M(z(t)) = \beta(z^2(t) - 1) \tag{1}$$

connected in series as displayed in Figure 1(b), which has been shown to be the simplest circuit capable of generating a one-scroll chaotic attractor. In order to generate a double-scroll and a four-scroll chaotic attractor Teng *et al.* [11] replaced the second-degree polynomial memristance by a fourth-degree polynomial memristance

$$M(z(t)) = \delta z^4(t) + \gamma z^2(t) - \beta,$$

and set the exponent of the internal state function of memristor to second order

$$\dot{z} = -i_L(t) - \alpha z(t) + i_L^2(t) z(t).$$

In this article, we investigate the bifurcation and chaos in a fractional-order version of the proposed memristor-based simplest chaotic circuit with two-degree polynomial memristance and a second-order exponent internal state.

2. SIMPLEST MEMRISTOR-BASED CHAOTIC CIRCUIT

The proposed simplest circuit in this article can generate a double-scroll (Figure 2(a)) and a four-scroll chaotic attractor (Figure 2(b)) by using only a second-degree polynomial memristance as in [10] and setting the exponent of the internal state function of the memristor to second order. The dynamic of the circuit is described by the mathematical model:

$$\begin{cases} \dot{x} &= ay, \\ \dot{y} &= -b(x + M(z)y), \\ \dot{z} &= -y - \alpha z + y^2 z, \end{cases} \tag{2}$$

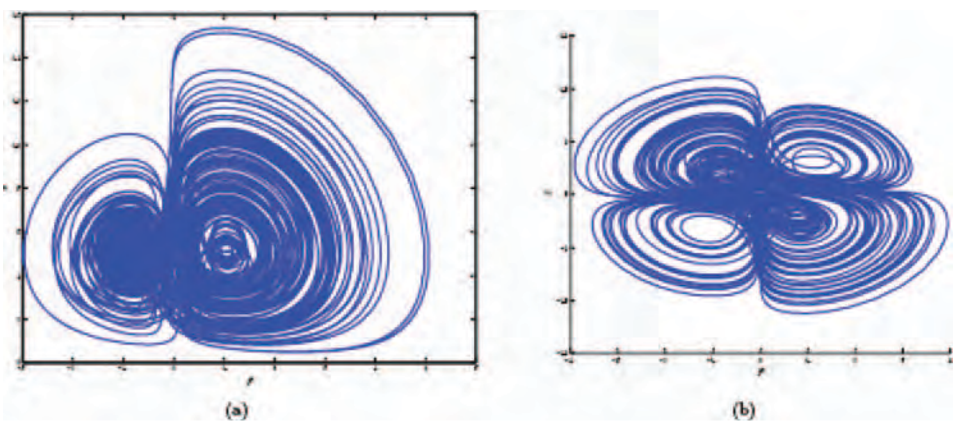

Figure 2. (a) Double-scroll chaotic attractor for $L = 3H$, $C = 1F$, $\alpha = 0.9$, $\beta = 10.1$, $\gamma = 0.4$. (b) Four-scroll chaotic attractor for $L = 3H$, $C = 1F$, $\alpha = 0.9$, $\beta = 3$, $\gamma = 0.4$.

where $x(t) = V(t)$ is the voltage across the capacitor, $y(t) = I_L(t)$ is the current through the inductor, $z(t)$ denotes the internal state variable of the memristor, $a = 1/C$ is the inverse capacitance, $b = 1/L$ is the inverse inductance and the memristor function is given by

$$M(z(t)) = \gamma z^2(t) - \beta.$$

The simulation of system (2) has been done using the fourth-order Runge–Kuta algorithm with the parameters values $L = 3H,\ C = 1F,\ \alpha = 0.9,\ \beta = 10.1$ and $\gamma = 0.4$ for Figure 2(a) and $L = 3H,\ C = 1F,\ \alpha = 0.9,\ \beta = 3$ and $\gamma = 0.4$ for Figure 2(b).

3. SIMPLEST FRACTIONAL-ORDER MEMRISTOR-BASED CHAOTIC CIRCUIT

In this article, we present the fractional-order memristor-based circuit and investigate its dynamics by mean of stability theory and numerical schemes.

3.1. Circuit Description and Fractional Model

In order to build the fractional-order memristor-based circuit we replace the electrical elements (capacitor, inductor and memristor) in the original circuit by its fractional version (fractional-order capacitor, fractional-order inductor and fractional-order memristor) (see Figure 3). Based on Curie's empirical law of 1889, Westerlund *et al.* proposed in 1994 a fractional-order linear capacitor model and a fractional-order inductor [12, 13].

For a general input voltage $V_{FC}(t)$ the current through the fractional-order capacitor is

$$I_F C(t) = C D^{q_1} V_{FC}(t),$$

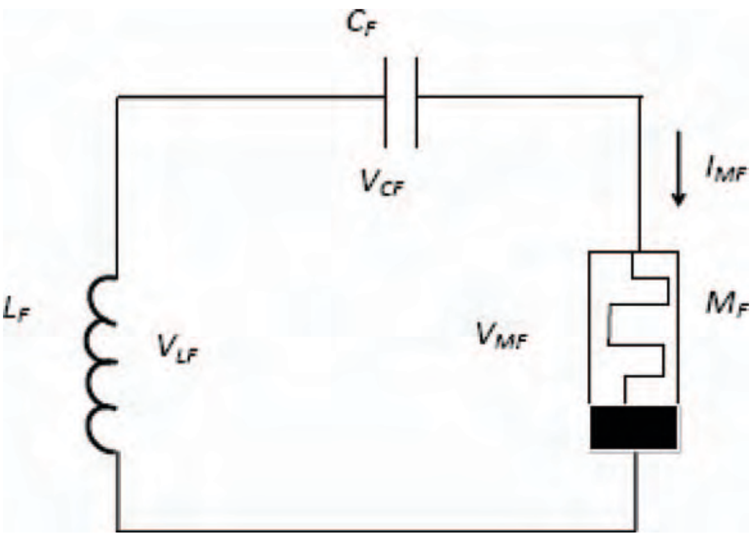

Figure 3. Example of a fractional-order circuit.

then

$$D^{q_1} V_{FC}(t) = \frac{1}{C} I_{FL}(t).$$

The constant q_1 is related to the losses of the capacitor. It should be noted that losses and dissipation are not always the same thing. Dissipation means generation of heat, instead losses stand for energy lost from the process under study but not necessarily in the form of heat [12].

For a general current through the fractional-order inductor the voltage is

$$V_{FL}(t) = L D^{q_2} I_{FL},$$

then

$$D^{q_2} I_{FL} = \frac{1}{L} V_{FL}(t).$$

The constant q_2 is related to the 'proximity effect'. When an alternating current flows through an electrical conductor, the current distribution is not uniform. One of the most important electromagnetic phenomena, which dramatically affects the current distribution within any current-carrying conductor, is the electromagnetic proximity effect. A table of various coils and their real orders q_2 is described in [14]. For a general current through the fractional-order memristor the voltage is [15]

$$\begin{cases} V_{FM} &= M(z(t)) i_{FM}(t), \\ D^{q_3} z(t) &= i_{FM}(t) - \alpha z(t) + i_{FM}^2 z(t). \end{cases} \tag{3}$$

Applying Kirchhoff's voltage law, we obtain

$$D^{q_2} i_{FL}(t) = -\frac{1}{L} \left(V_{FC}(t) + M(z(t)) i_{FL}(t) \right).$$

Using the previous notations of state variable, we obtain

$$\begin{cases} D^{q_1} x &= ay, \\ D^{q_2} y &= -b(x + M(z)y), \\ D^{q_3} z &= -y - \alpha z + y^2 z, \end{cases} \tag{4}$$

Proposition 1. The system (4) is invariant under the transformation $T : (x, y, z) \to (-x, -y, -z)$.

Proof. Suppose that $(x(t),\ y(t),\ z(t))$ is a solution of system (4). Multiplying both sides of Equation (4) by -1 and taking into account the linearity property of the fractional derivative

$$(-D^{q_1} x(t) = D^{q_1}(-x(t)), \quad -D^{q_2} y(t) = D^{q_2}(-y(t)), \quad -D^{q_3} z(t) = D^{q_3}(-z(t)),)$$

we obtain

$$\begin{cases} D^{q_1}(-x) &= a(-y), \\ D^{q_2}(-y) &= -b(-x + M(-z)(-y)), \\ D^{q_3}(-z) &= -(-y) - \alpha(-z) + (-y)^2(-z). \end{cases} \tag{5}$$

then $(-x(t), -y(t), -z(t))$ is a solution of Equation (4).

The following corollary is a direct consequence of this proposition

Corollary 1. If for a given values of the parameter of system (4) there exists a non-symmetrical attractor (regular or chaotic) with respect to the origin $(0,\ 0,\ 0)$, then there is a coexistence of at last two attractors which are symmetric to each other with respect to the origin.

3.2. Stability Analysis

In this subsection the parameters are set to $a = 1$, $b = 1/3$, $\alpha = 0.9$, $\gamma = 0.1$ with $\beta > 0$. We consider the case where all the fractional orders are set to the same value $q_1 = q_2 = q_3 = q \in]0,\ 2[$they are considered as control parameters. By setting the left-hand side of Equation (4) to zero, we obtain the origin as the only one equilibrium point$E = (0,\ 0,\ 0)$. The stability of E can be investigated using the theorem 2 in [16] and the proposition 2.3 in [17].

Theorem 3.1. The fractional-order system (4) is asymptotically stable if all the eigenvalues λ of the Jacobian matrix J satisfy the condition

$$|\arg(\lambda)| > \frac{q\pi}{2}.$$

The Jacobian matrix of system (4) at E is $\begin{pmatrix} 0 & 1 & 0 \\ -\frac{1}{3} & \frac{\beta}{3} & 0 \\ 0 & -1 & -0.9 \end{pmatrix}$.

Its characteristic equation is

$$\lambda^3 - (\frac{\beta}{3} - 0.9)\lambda^2 + \frac{1-\beta}{3}\lambda + 0.3 = 0,$$

or equivalently

$$(\lambda + 0.9)(\lambda^2 - \frac{\beta}{3}\lambda + \frac{1}{3}) = 0.$$

The eigenvalues are $\lambda_1 = -\ 0.9 < 0$ and

- if $\beta \in [2\sqrt{3}, +\infty[$, then $\lambda_{2,\,3} = \frac{\beta \pm \sqrt{\beta^2 - 12}}{6} > 0$, in this case E is unstable for every value of the commensurate order $q \in]0,\ 2[$, or,
- if $\beta \in]0,\ 2\sqrt{3}[$, then $\lambda_{2,\,3} = \frac{\beta \pm j\sqrt{12-\beta^2}}{6}$, in this case E is asymptotically stable for the values of q and β satisfying, $q < \frac{2}{\pi}\left|\tan^{-1}\left(\frac{\sqrt{12-\beta^2}}{\beta}\right)\right|$ and unstable for the values of q and β satisfying $q > \frac{2}{\pi}\left|\tan^{-1}\left(\frac{\sqrt{12-\beta^2}}{\beta}\right)\right|$.

The stable and unstable regions in the ($\beta - q$) plane (Figure 4) are separated by the curve of equation $q = \frac{2}{\pi}\left|\tan^{-1}\left(\frac{\sqrt{12-\beta^2}}{\beta}\right)\right|$.

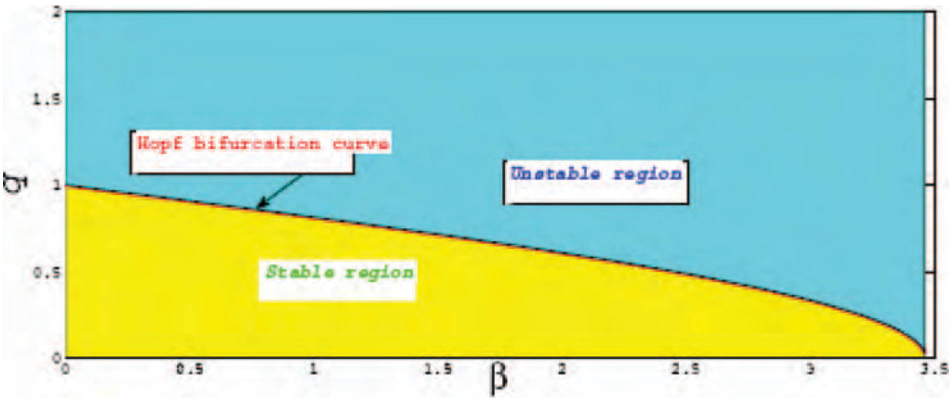

Figure 4. Stability region of the fractional-order system (4) in the $(\beta - q)$ plane

3.3. Bifurcation Analysis

In [18], a fractional-order Hopf bifurcation condition is proposed which states that system (4) undergoes a Hopf bifurcation through the equilibrium E at the value β^* of β if:

(i) the Jacobian matrix has two complex–conjugate eigenvalues $\lambda_{2,3}$ and one real $\lambda_1 < 0$,

(ii) $m_{2,3}(q, \beta^*) = 0$,

(iii) $\left.\dfrac{\partial m_{2,3}}{\partial \beta}\right|_{\beta=\beta^*} \neq 0$,

where

$$m_i(q,\ \beta) = q\frac{\pi}{2} - |\arg(\lambda_i(\beta))|\,, \quad i = 1,\ 2,\ 3.$$

If $\beta \in]0,\ 2\sqrt{3}[$. then the first condition is satisfied. Namely, we have $\lambda_1 = -0.9 < 0$ and $\lambda_{2,3} = \frac{\beta \pm j\sqrt{12-\beta^2}}{6}$.

For β^* solution of $m_{2,3}(q,\ \beta^*) = 0$ we have

$$\left.\frac{\partial m_{2,3}}{\partial \beta}\right|_{\beta=\beta^*} = \left(\frac{1}{1 + \frac{12-(\beta^*)^2}{(\beta^*)^2}}\right)\left(\frac{-24}{2(\beta^*)^2\sqrt{12-(\beta^*)^2}}\right) \neq 0.$$

Then, all the proposed conditions are satisfied for every solution of $m_{2,3}(q,\ \beta^*) = 0$.

For example if $q = 0.92$, then, $\beta^* = 0.4342$ is a Hopf bifurcation point.

If we consider the fractional order q as a control parameter then we have

$$\left.\frac{\partial m_{2,3}}{\partial q}\right|_{q=q^*} = \frac{\pi}{2} \neq 0.$$

Hence, all the solutions q^* of $m_{2,3}(q^*,\ \beta) = 0$ with $\beta \in]0,\ 2\sqrt{3}[$ are Hopf bifurcation points.

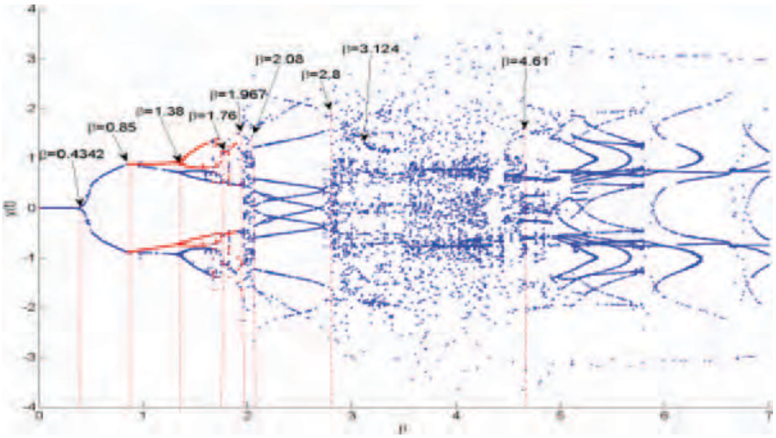

Figure 5. Bifurcation versus the parameter β for $q = 0.92$

For example, if $\beta = 3.3$, we obtain $q^* = 0.1967$ which is a Hopf bifurcation point. In order to illustrate the above-mentioned conditions we present some numerical results.

3.3.1. Bifurcation versus the parameter β

Figure 5 illustrates the bifurcation diagram of y versus the parameter β over the range $0 < \beta \leq 7$, where the fractional order is $q = 0.92$. The discretisation of the system is done using the Poincaré section $\Sigma_1 = \{(x,\ y) \in R^2/z = 0\}$ for $0 < \beta \leq 2.08$, the Poincaré sections $\Sigma_2 = \{(x,\ y) \in R^2/z = 5\}$ and $\Sigma_3 = \{(x,\ y) \in R^2/z = -5\}$ for $2.08 < \beta \leq 7$.

From this figure, we can see that when $0 < \beta \leq 0.4342$, the equilibrium point E is locally asymptotically stable (stationary behaviour) (see Figure 6(a), when, $0.4342 < \beta < 1.98$ the equilibrium point E is unstable and the system exhibits a periodic behaviour (Figure 6(b)), which is in agreement with the theoretical results; furthermore, the cycle created via Hopf bifurcation bifurcates in turn when $\beta = 0.85$ and two period-1 limit cycles appear (coexistence of two period-1 limit cycles for $\beta \in]0.85,\ 1.38[$ as shown in Figure 6(c)), and these two period-1 limit cycles bifurcate in turn when $\beta = 1.38$ and two period-2 limit cycles appear (coexistence of two period-2 limit cycles for $\beta \in]1.38,\ 1.76[$ as shown in Figure 6(d)). Another bifurcation occurs at $\beta = 1.76$ where the two period-2 limit cycles become two period-1 limit cycles, these two limit cycles disappear at $\beta = 1.967$ and are replaced by a four scroll chaotic attractor. The chaotic behaviour is observed for $\beta \in]1.967,\ 2.08[\cup]2.8,\ 4.6]$ (Figures 6(e), (g), (i)), alternated with a periodic behaviour for $\beta \in]2.08,\ 2.8[$, $\beta > 4.6$ and for β near the values 3.124 (Figures 6(f), (h), (j)), here note that for $\beta \in]4.43,\ 4.6[$ there is coexistence of two 2-scroll chaotic attractors, (Figure 6(i)) and for β near the values 5.22 there is coexistence of four periodic orbits, (Figure 6(j)). The four initial conditions used in this numerical computation are $(-1.3112,\ 0.4170,\ 14.7214)$, $(1.5092,\ 0.3829,\ -14.1774)$, $(-1.5092,\ -0.3829,\ 14.1774)$ and $(1.3112,\ -0.4170,\ -14.7214)$.

3.3.2. Bifurcation versus the parameter q

Figure 7 illustrates the bifurcation diagram of y versus the fractional order q over the range$0 < q \leq 1.7$. The discretisation of the system is done using the Poincaré section $\Sigma_1 = \{(x,\ y) \in R^2/z = 0\}$;

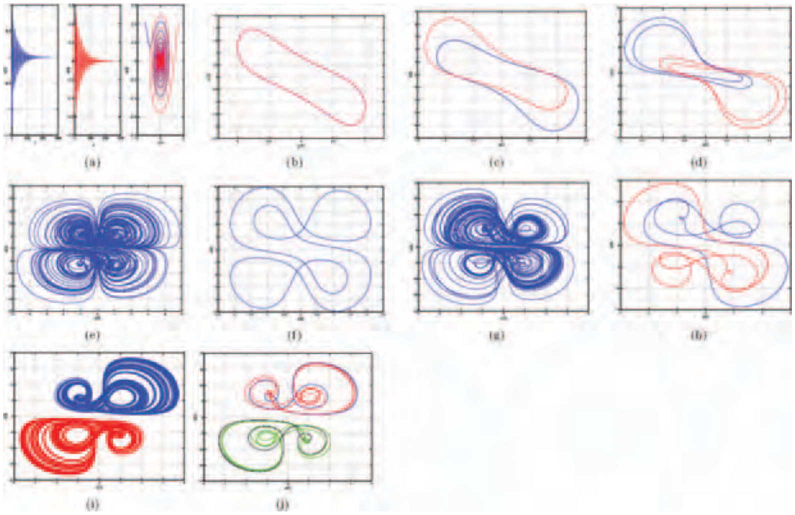

Figure 6. Phase portraits of the fractional-order system (4) for $q = 0.92$ and (a) $\beta = 0.3$, (b) $\beta = 0.6$, (c) $\beta = 0.9$, (d) $\beta = 1.5$, (e) $\beta = 2$, (f) $\beta = 2.5$, (g) $\beta = 2.9$ (h) $\beta = 3.124$, (i) $\beta = 4.6$, (j) $\beta = 5.22$

in this figure we can see that when $0 < q < 0.1967$, the equilibrium point E is locally asymptotically stable (stationary behaviour) (Figure 9(a)), when $q \approx 0.1967$, the equilibrium point E losses its stability and the system exhibits a periodic behaviour until $q \approx 0.8216$, which is in agreement with the theoretical results.

We can distinguish some intervals of periodicity. The first one is $q \in [0.1967,\ 0.8]$, where one period-1 limit cycle appears (Figure 9(b)).

To distinguish the other interval we draw another bifurcation diagram of x versus the fractional order q over the range $0.8 < q \leq 0.83$ (Figure 8(b)). The discretisation of the system is done

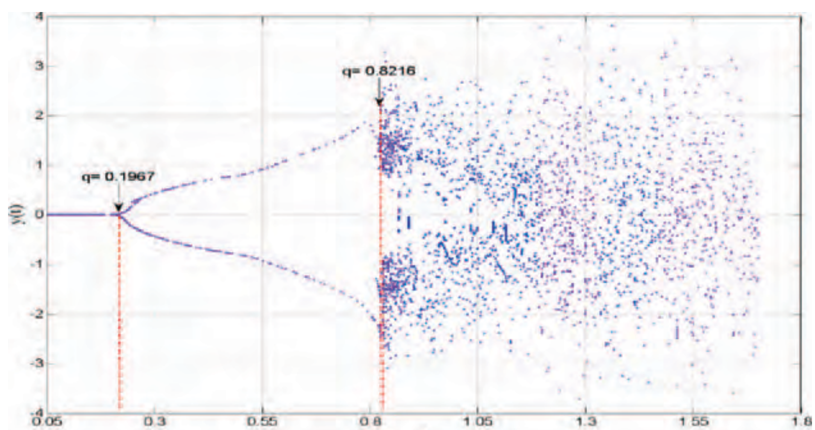

Figure 7. Bifurcation versus the fractional order q for $\beta = 3.3$

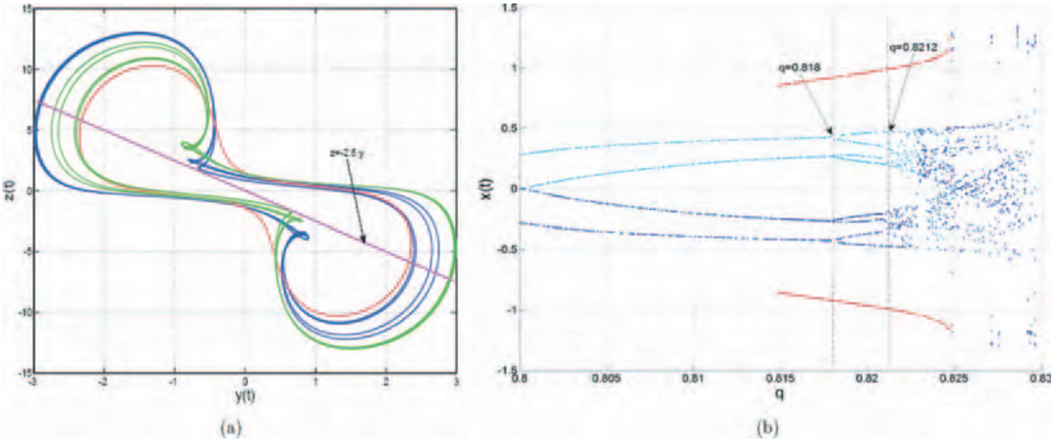

Figure 8. (a) Poincaré section $\Sigma = \left\{(x,\ y,\ z) \in R^3/z = -\frac{5}{2}y\right\}$. (b) Bifurcation versus the fractional order q for $\beta = 3.3$

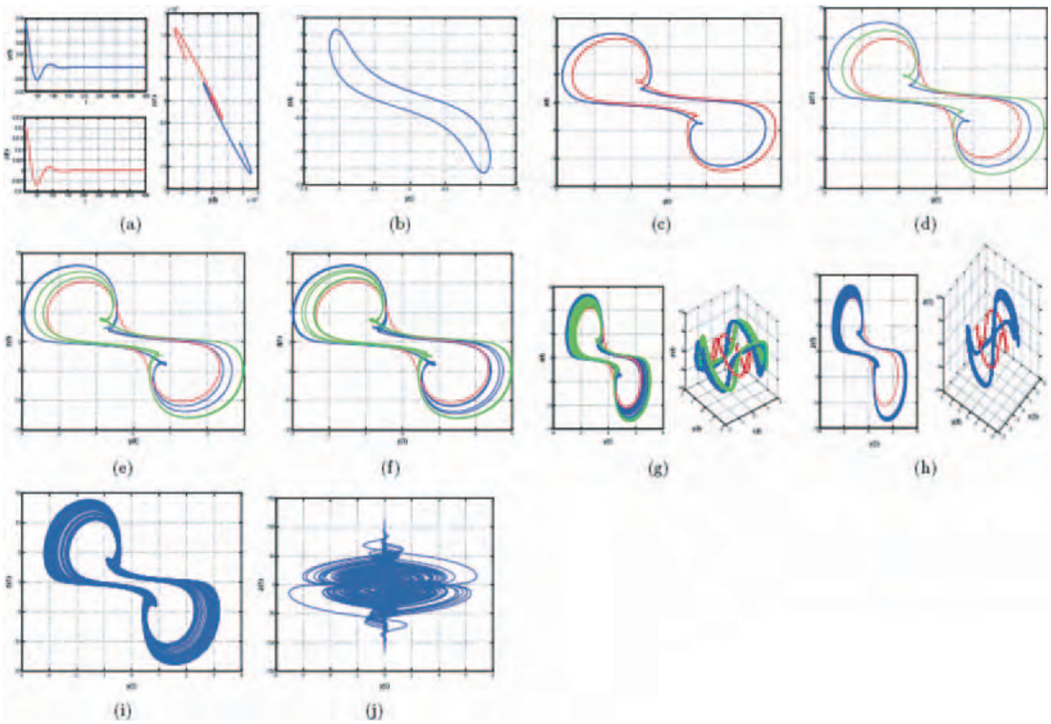

Figure 9. Phase portraits of the fractional-order system (4) for $\beta = 3.3$ and (a) $q = 0.16$, (b) $q = 0.3$, (c) $q = 0.81$, (d) $q = 0.816$, (e) $q = 0.82$, (f) $q = 0.8212$, (g) $q = 0.8225$, (h) $q = 0.823$, (i) $q = 0.825$, (j) $q = 1.5$

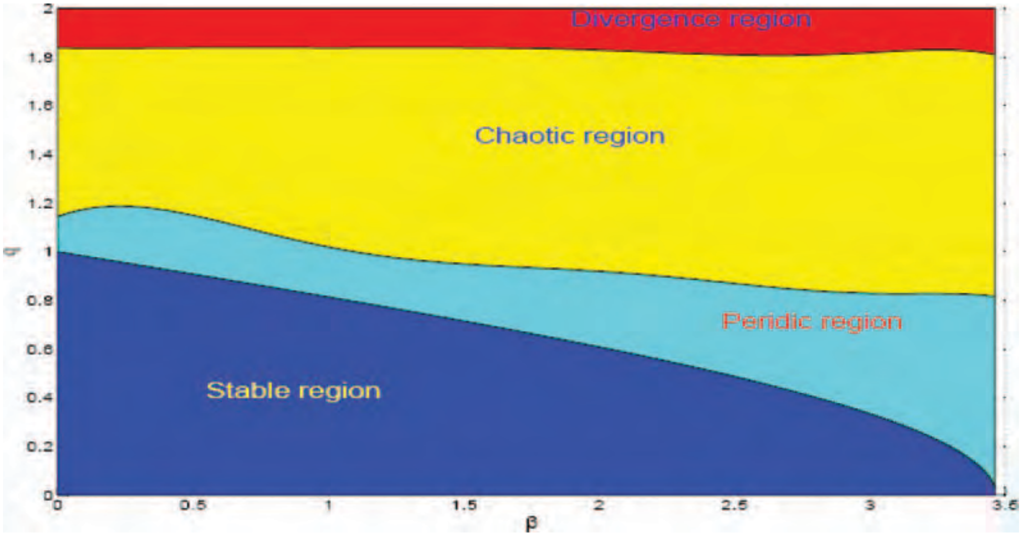

Figure 10. Bifurcation curves of the fractional-order system (4) in the $(\beta - q)$ plane

using the Poincaré section $\Sigma = \left\{(x,\ y,\ z) \in R^3/z = -\frac{5}{2}y\right\}$ (Figure 8(a)); in this bifurcation diagram we can see that the second interval of periodicity is $q \in [0.8,\ 0.814]$, in which two period-1 limit cycles coexist (Figure 9(c)). Another similar interval is $q \in [0.815,\ 0.818]$ where three period-1 limit cycles coexist (Figure 9(d)). In the interval $q \in [0.818,\ 0.821]$ two period-2 limit cycles and one period-1 limit cycle coexist (Figure 9(e)). The period-1 limit cycle persists until $q \approx 0.825$ but the period-2 limit cycles bifurcate towards a two period-4 limit cycles for $q \approx 0.8212$ (Figure 9(f)). This process of period doubling is continued until $q \approx 0.8217$ where two chaotic attractors appear and coexist with the period-1 limit cycle (Figure 9(g)). The two chaotic attractors collide and give a new chaotic attractor for $q \approx 0.823$ which coexists with the period-1 limit cycle (Figure 9(h)), until $q \approx 0.825$ where the period-1 limit cycle disappears, (Figure 9(i)). For $q \geq 0.825$ there is a chaotic behaviour (the system can display a double-scroll chaotic attractor or a four-scroll chaotic attractor) which alternates with a periodic behaviour, for example at $q \approx 0.86$ two limit cycles coexist, for $q \in [0.89,\ 0.9]$ one limit cycle appears and at $q \approx 0.92$ two limit cycles coexist. For $q \geq 0.93$ the system displays only a four-scroll chaotic attractor which changes its form continuously so one obtains a new chaotic attractor not observed in the integer order case (Figure 9(j)).

In order to investigate the dynamics in the $(\beta - q)$ plane we determine the smallest value q_c of q for which the system exhibits a chaotic motion and the smallest value q_d of q for which we have a divergence. First, the critical values are determined for eight values of the parameter β as represented in Table 1, then using Lagrange polynomial interpolation we approximate all critical values $q_c(\beta)$ and $q_d(\beta)$ for $\beta \in [0,\ 2\sqrt{3}]$, as illustrated in Figure 10.

3.4. The 0–1 Test for Detecting the Chaos

An efficient binary test for chaos, called '$0 - 1$ test', has been recently proposed [19] and applied to fractional systems in [20]. The idea underlying the test is to construct a random walk-type

Table 1. Critical values q_c for the chaotic motion and q_d for the divergence

β	q_c	q_d
0.01	1.145	1.84
0.5	1.15	1.84
1	1.02	1.84
1.5	0.95	1.84
2	0.92	1.83
2.5	0.87	1.81
3	0.83	1.82
$2\sqrt{3}$	0.81	1.80

process from the data and then to examine how the variance of the random walk scales with time. Specifically, consider a set of discrete data, sampled at times $n = 1,\ 2,\ 3, ...,$ representing a one-dimensional observable data set obtained from the system dynamics, this algorithm consists of the following steps:

(i) Choose a random value $c \in \left(\frac{\pi}{5}, \frac{4\pi}{5}\right)$ and define the new coordinates as follows:

$$P_c(n) = \sum_{j=1}^{n} \phi(j) \cos(\theta(j)),$$

and

$$Q_c(n) = \sum_{j=1}^{n} \phi(j) \sin(\theta(j)).$$

where $\theta(j) = jc + \sum_{i=1}^{j} \phi(i), \quad j = 1,\ 2,\ 3, ...n.$

(ii) Compute the mean square displacement as follows:

$$M_c(n) = \lim_{N} \to \infty^{N}$$

where $n \in \left[1, \frac{N}{10}\right]$.

(iii) Define $K = median(K_c)$ where

$$K_c = \frac{cov(\xi,\ \Delta)}{\sqrt{var(\xi)var(\Delta))}} \in [-1,\ 1],$$

with

$$\xi = (1,\ 2,\ 3, \ldots n_{cut}), \quad \Delta = (M_c(1),\ M_c(2), \ldots M_c(n_{cut})),$$

and $n_{cut} = round(\frac{N}{10})$.

(iv) Interpret outputs: when K is close to 0, the motion is classified as regular (i.e. periodic or quasi-periodic) and when K is near 1, the motion is classified as chaotic.

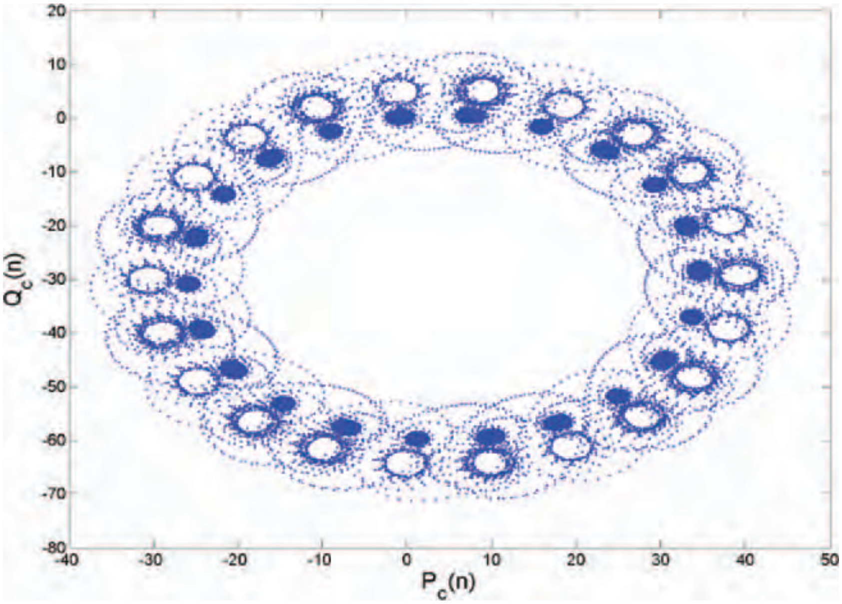

Figure 11. Bounded trajectories indicating regular dynamic for $\beta = 3.3$ and $q = 0.81$

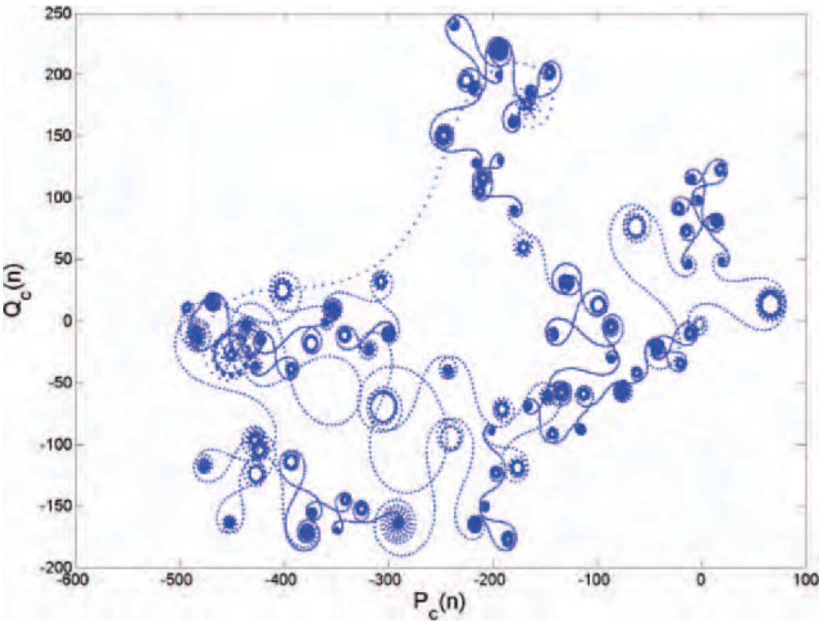

Figure 12. Unbounded Brownian-like trajectories indicating chaos for $\beta = 3.3$ and $q = 1.5$

Besides the computation of the rate K, the inspection of the dynamics of the $(P_c(n),\ Q_c(n))$trajectories provides a simple visual test of whether the system dynamics is chaotic or not. Namely, bounded trajectories in the $(P_c(n),\ Q_c(n))$ plane imply regular dynamics, whereas Brownian-like (unbounded) trajectories imply chaotic dynamics [19]. In order to analyse the dynamic of the fractional system (4), the '$0-1$ test' has been applied directly to the time series data.

For $\beta = 3.3$ and $q = 0.81$, one obtains $K = 0.0085 \approx 0$. Then the dynamics is regular. Moreover, Figure 11 depicts bounded trajectories in the $(P_c(n),\ Q_c(n))$ plane.

For $\beta = 3.3$ and $q = 1.5$, one obtains $K = 0.9162 \approx 1$. Then the dynamics is chaotic. Moreover, Figure 12 depicts Brownian-like (unbounded) trajectories in $(P_c(n),\ Q_c(n))$ plane.

4. CONCLUSION

In this work, we have investigated the dynamical behaviours of the simplest fractional-order electrical circuit which utilises only three elements in series including a memristor. A second-degree polynomial memristance and a second-order exponent internal state are used in this circuit to increase the complexity of the attractor. Coexistence of four limit cycles and coexistence of one (and two) chaotic attractor with one limit cycle are reported. A theoretical analysis of the system dynamics has been performed using phase portraits, bifurcation diagrams and the $0-1$ test which has confirmed the presence of chaos in the considered system.

REFERENCES

[1] Cafagna, D., 2007. "Fractional Calculus: A Mathematical Tool from the Past for Present Engineers", *IEEE Industrial Electronic Magazine,* 1, pp. 35–40.

[2] Hilfer, R., 2000. *Applications of Fractional Calculus in Physics.* World Scientific, Singapore.

[3] Sun, H., Abdelwahed, A. and Onaral, B., 1984. "Linear Approximation for Transfer Function with a Pole of Fractional Order", *IEEE Transactions on Automatic. Control,* 29, pp. 441–444.

[4] Podlubny, I., 1999. *Fractional Differential Equations*. Academic Press, San Diego.

[5] Tavazoei, M. S. and Haeri, M., 2009. "A Proof for Non-Existence of Periodic Solutions in Time Invariant Fractional Order Systems", *Automatica,* 45, pp. 1886–1890.

[6] Abdelouahab, M-S. and Hamri, N., 2015. "The Grünwald-Letnikov Fractional-Order Derivative with Fixed Memory Length", *Mediterranean Journal of Mathematics*, doi 10.1007/s00009-015-0525-3, pp. 1–16.

[7] Chua, L. O., 1971. "Memristor—The Missing Circuit Element", *IEEE Transactions on Circuit Theory,* 18, pp. 507–519.

[8] Strukov, D. B., Snider, G. S., Stewart, D. R. and Williams, R. S., 2008. "The Missing Memristor Found", *Nature,* 453, pp. 80–83.

[9] Abdelouahab, M-S., Lozi, R. and Chua, L.O., 2014. "Memfractance: A Mathematical Paradigm for Circuit Elements with Memory", *International Journal of Bifurcation and Chaos*, 24(9), 29 p.

[10] Muthuswamy, B. and Chua, L. O., 2010. "Simplest Chaotic Circuit", *International Journal of Bifurcation and Chaos,* 20(5), pp. 1567–1580.

[11] Teng, L., Iu, H. H. C. and Wang, X., 2014. "Chaotic Behavior in Fractional-Order Memristor-Based Simplest Chaotic Circuit Using Fourth Degree Polynomial", *Nonlinear Dynamics,* 77, pp. 231–241.

[12] Westerlund, S. and Ekstam, S., 1994. "Capacitor Theory", *IEEE Transactions on Dielectrics and Electrical Insulation,* 1(5), pp. 826–839.

[13] Westerlund, S., 2002. *Dead Matter Has Memory*!, Causal Consulting, Kalmar, Sweden.

[14] Schafer, I. and Kruger, K., 2008. "Modelling of Lossy Coils Using Fractional Derivatives", *Journal of Physics D: Applied Physics,* 41, pp. 1–8.

[15] Coopmans, C., Petras, I. and Chen, Y. Q., 2009. “Analogue Fractional-Order Generalized Memristive Devices”, *Proceedings of the ASME International Design Engineering Technical Conferences and Computers and Information in Engineering Conference*, IDETC/CIE 2009 August 30–September 2, 2009, San Diego, California, USA, DETC 2009-86861.

[16] Cafagna, D. and Grassi, G., 2012. “On the Simplest Fractional-Order Memristor-Based Haotic System”, *Nonlinear Dynamics,* 70, pp. 1185–1197.

[17] Abdelouahab, M-S., Hamri, N. and Wang, J., 2010. “Chaos Control of a Fractional-Order Financial System”, *Mathematical Problems in Engineering,* doi:10.1155/2010/270646, 18 pages.

[18] Abdelouahab, M-S., Hamri, N. and Wang, J., 2012. “Hopf Bifurcation and Chaos in Fractional-Order Modified Hybrid Optical System”, *Nonlinear Dynamics,* 69, pp. 275–284.

[19] Gottwald, G. A. and Melbourne, I., 2004. “A New Test for Chaos in Deterministic Systems”, *Proceedings of Royal Society London,* A, 460, pp. 603–611.

[20] Cafagna, D. and Grassi, G., 2009. “Hyperchaos in the Fractional-Order Rössler System with Lowest-Order”, *International Journal of Bifurcation and Chaos.*, 19, pp. 339–347.